Tellus
SERIES A
DYNAMIC
METEOROLOGY
AND OCEANOGRAPHY
PUBLISHED BY THE INTERNATIONAL METEOROLOGICAL INSTITUTE IN STOCKHOLM

Tellus (2011), 63A, 24–40

TELLUS

21st century changes in the European climate: uncertainties derived from an ensemble of regional climate model simulations

By ERIK KJELLSTRÖM*, GRIGORY NIKULIN, ULF HANSSON, GUSTAV STRANDBERG and ANDERS ULLERSTIG, *Rossby Centre, Swedish Meteorological and Hydrological Institute, SE 601 96 Norrköping, Sweden*

(Manuscript received 18 December 2009; in final form 18 June 2010)

ABSTRACT

Seasonal mean temperature, precipitation and wind speed over Europe are analysed in an ensemble of 16 regional climate model (RCM) simulations for 1961–2100. The RCM takes boundary conditions from seven global climate models (GCMs) under four emission scenarios. One GCM was run three times under one emission scenario differing only in initial conditions. The ensemble is used to; (i) evaluate the simulated climate for 1961–1990, (ii) assess future climate change and (iii) illustrate uncertainties in future climate change related to natural variability, boundary conditions and emissions. Biases in the 1961–1990 period are strongly related to errors in the large-scale circulation in the GCMs. Significant temperature increases are seen for all of Europe already in the next decades. Precipitation increases in northern and decreases in southern Europe with a zone in between where the sign of change is uncertain. Wind speed decreases in many areas with exceptions in the northern seas and in parts of the Mediterranean in summer. Uncertainty largely depends on choice of GCM and their representation of changes in the large-scale circulation. The uncertainty related to forcing is most important by the end of the century while natural variability sometimes dominates the uncertainty in the nearest few decades.

1. Introduction

There are a number of fundamental uncertainties in our understanding of climate change in the 21st century. These can be summarized into terms of three questions: (i) how will the external forcing of the climate system change in the future? (ii) how will changes in external forcing factors influence climate? (iii) to what degree is the future climate change signal masked/amplified by natural variability of the climate system? A common way to deal with these uncertainties is to perform several simulations constituting an ensemble (e.g. Christensen et al., 2007). Such ensembles, on finer spatial scales utilizing information from regional climate models (RCMs), have been developed in the European projects PRUDENCE (e.g. Christensen and Christensen, 2007; Déqué et al., 2007; Jacob et al., 2007; Haugen and Iversen, 2008) and ENSEMBLES (Hewitt and Griggs, 2004; van der Linden and Mitchell, 2009). An ensemble can be used to illustrate uncertainties on the regional scale or to derive probabilistic climate change information in a region. The specific uncertainties (i)–(iii) are handled similarly by performing several simulations. Hence, several different emission scenarios are used to get a grip on the uncertainty related to external forcing thereby sampling a multitude of possible outcomes such as those described in the Special Report on Emission Scenarios (SRES, Nakićenović and Swart, 2000). Similarly, by using multiple climate models or an ensemble of simulations with one model perturbed in its formulation of the physics, parts of the uncertainties related to how changes in forcing influence the climate can be assessed (e.g. Meehl et al., 2007; Murphy et al., 2007). Finally, to get a grip on the natural variability one may use several simulations with one climate model under the same emission scenario differing only in initial conditions similar to what is done in seasonal prediction or at the numerical weather prediction centres (e.g. Palmer et al., 2004; Sterl et al., 2008).

Earlier studies have shown that a large fraction of the uncertainties in regional climate change simulations is connected to which global climate model (GCM) that is used for deriving the regional information (e.g. Hawkins and Sutton, 2009). Downscaling methods, including RCMs and statistical downscaling, preserves most large-scale features from the GCMs. These results apply for seasonal mean changes in temperature

*Corresponding author.
e-mail: erik.kjellstrom@smhi.se
DOI: 10.1111/j.1600-0870.2010.00475.x

and precipitation for large areas in Europe (Räisänen et al., 2004; Déqué et al., 2007). The GCMs determine a large part of the climate change signal also at finer temporal and spatial scales. Part of the uncertainty is connected to choice of downscaling method, in particular that related to higher order variability and extremes. In terms of regional climate modelling this means choice of RCM or parametrization schemes used in them. Examples of large dependence on choice of RCM have been shown for daily temperature statistics (Kjellström et al., 2007), precipitation (Beniston et al., 2007) and wind speed (Rockel and Woth, 2007).

A drawback with earlier regional climate change ensembles is that the number of forcing GCMs has been restricted (mainly one in PRUDENCE), or that single RCMs only have downscaled a few GCMs (up to three in ENSEMBLES). At the Rossby Centre a 16-member ensemble of transient regional climate change scenarios at 50 km horizontal resolution for the time period 1961–2100 has been developed. Six of these simulations, downscaling different GCMs under the same emission scenario, have been analysed in terms of daily variability, including 20-yr return values of extreme events of maximum and minimum temperatures, precipitation and wind speed by Nikulin et al. (2011). Here, we focus on seasonal mean changes in mean sea level pressure (MSLP), 2-m temperature (T_{2m}), precipitation (P) and 10-m wind speed (W_{10m}) to illustrate the spread in average climate conditions by the end of the century (2071–2100) for Europe. Further, we make use of the full 16-member ensemble that also holds a number of different emission scenarios and simulations differing only in initial conditions to illustrate how natural variability, choice of driving GCMs and choice of emission scenarios contributes to the spread at different future time periods starting from the nearest decades.

2. Model and experiments

2.1. The Rossby Centre regional climate model RCA3

RCA3 is a RCM that contains a full description of the atmosphere and its interaction with the land surface. It includes a land surface model (Samuelsson et al., 2006) and a lake model, PROBE (Ljungemyr et al., 1996). Sea-surface temperature (SST) and sea-ice conditions are prescribed for all ocean areas within the chosen model domain including the Baltic Sea for the present set-up. Given realistic boundary conditions, such as the reanalysis products ERA15 (Gibson et al., 1997) and ERA40 (Uppala et al., 2005), RCA3 and its predecessor RCA2 reproduce many observed climate conditions on the regional scale including seasonal mean temperatures, water fluxes and snow cover (Jones et al., 2004, Kjellström et al., 2005; Lind and Kjellström, 2009; Samuelsson et al., 2011). Deviations from observations also exist such as a warm bias in winter in parts of the northeastern domain and an overestimation of P in parts of northern Europe in summer as presented below. Such biases are seen also in other state-of-the-art RCMs (e.g. Christensen et al., 2007). Further documentation of RCA3 and a more detailed description of its performance in the recent past climate can be found in Samuelsson et al. (2011).

In the experiments used here RCA3 was run at $0.44^\circ \times 0.44^\circ$ (approximately 50 km $\times$ 50 km) horizontal resolution with 24 levels up to 10 hPa in the vertical direction at a time step of 30 min. The set up covers Europe and we present results from the interior model domain excluding the eight-point boundary relaxation zones in all directions (e.g. Fig. 1).

2.2. Model evaluation

Although model evaluation is not the scope of this paper some comparisons of model results to the observed climate in the late–20th-century are presented. The rationale is to illustrate how large biases a state-of-the-art RCM shows, both when forced by perfect boundary conditions and when forced by lateral boundary conditions from GCMs. By perfect boundary conditions, we here mean the European Centre for Medium range Weather Forecasts (ECMWF) reanalysis product ERA40. More results from these perfect boundary experiments can be found in Samuelsson et al. (2011) presenting a more comprehensive model evaluation.

Model results are compared to a gridded observational data set (E-OBS) recently derived within the European ENSEMBLES project. The data set is based on daily data extending back to 1960 (Haylock et al., 2008; Klok and Klein Tank, 2008). A benefit from using this particular data set is that it has been constructed to represent grid box average observations allowing direct comparison to model results. In addition, no further interpolation is needed because the E-OBS data set is on the same grid that is used in RCA3. Here, we calculate seasonal and annual averages of T_{2m} and P based on the daily data. For MSLP and W_{10m} there are no independent data sets to compare with. For MSLP we compare simulated results to ERA40 data. This is not possible for W_{10m}, as the relatively coarse resolution in the ECMWF model tends to imply biased wind speeds, in particular in areas including complex terrain mountainous regions (Barstad et al., 2008). For W_{10m} we do not perform any comparison to observations in the control period but merely present the climate change signal.

2.3. Boundary data from GCMs and emission scenarios

The Rossby Centre ensemble of regional climate change scenarios at 50 km horizontal resolution is presented in Table 1. It consists of sixteen 140-yr transient climate change simulations covering the time period 1961–2100. Differences between the different simulations are that they use different GCMs for providing boundary conditions, different emission scenarios and/or different initial conditions. The GCMs that are fully coupled atmosphere–ocean general circulation models are forced by different emission scenarios from SRES (Nakićenović and Swart,

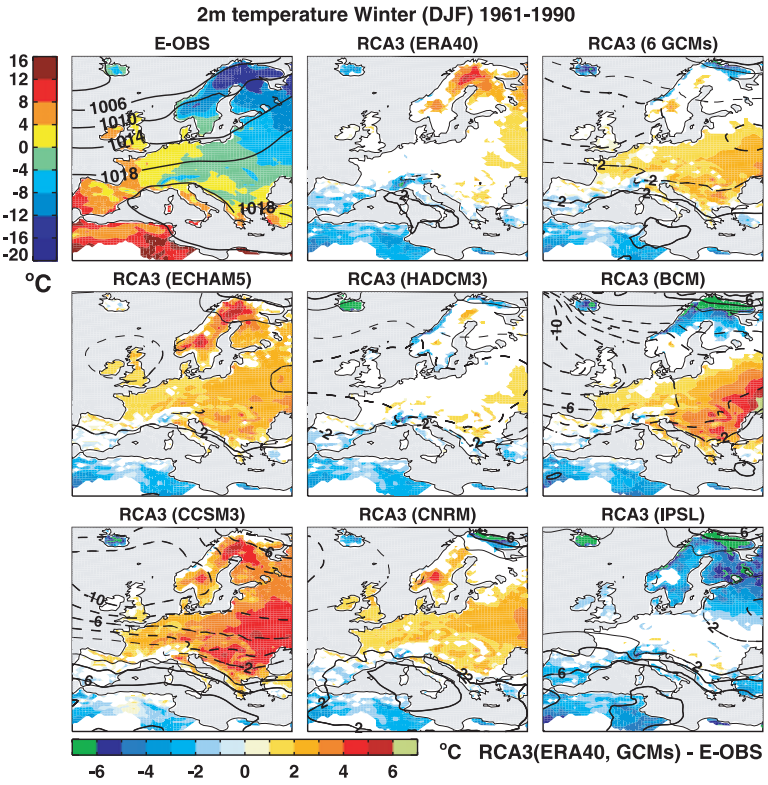

Fig. 1. (top, left-hand panel) Winter (DJF) mean T_{2m} (colour, °C, E-OBS) and MSLP (hPa, ERA40) and biases of T_{2m} and MSLP in the RCA3 simulations driven by (top, middle) the ERA40 reanalysis, (middle and bottom rows) six different GCMs and (top, right-hand panel) their ensemble mean. Only T_{2m} differences significant at the 5% significance level are shown. Correspondingly, statistically significant differences for MSLP are indicated with thick lines.

Table 1. Simulations in the regional climate change ensemble at the Rossby Centre

No	GCM (name used in text)	Emission scenario	Reference
1	CNRM-CM3 (CNRM)	*A1B*	Gibelin and Déqué (2003)
2	BCCR-BCM2.0 (BCM)	*A1B*	Déqué et al. (1994); Bleck et al. (1992)
3	CCSM3 (CCSM3)	A2	Collins et al. (2006)
4		*A1B*	
5		B2	
6	ECHAM4/OPYC3 (ECHAM4)	A2	Roeckner et al. (1999)
7		B2	
8	ECHAM5/MPI-OM (ECHAM5)	A2-r1	
9		A1B-r1	Roeckner et al. (2006),
10		A1B-r2	Jungclaus et al. (2006)
11		*A1B-r3*	
12		B1-r1	
13	HadCM3 (HadCM3)	*A1B-ref*	Gordon et al. (2000)
14		A1B-low	
15		A1B-high	
16	IPSL-CM4 (IPSL)	*A1B*	Hourdin et al. (2006)

Note: All simulations are transient and cover the time period 1961–2100. The six simulations in italics are the ones constituting the A1B-ensemble used in most of the figures.

2000). In particular, we present results from six simulations with different GCMs all under the SRES A1B emission scenario. Further, one GCM (ECHAM5) has been used to simulate the A1B emission scenario three times differing only in initial conditions to sample some of the natural variability (these three are labelled '-r1', '-r2' and '-r3' in the following). The A2 and B2 simulations with ECHAM5 both use the '-r1' starting conditions, implying that there is one three-member ensemble downscaling ECHAM5-r1 differing only in emission scenario. Another GCM (HadCM3) has been run with three different parameter settings to sample some of the uncertainty related to model formulation (Collins et al., 2010). That particular ensemble of three

simulations includes the reference version of the HadCM3 model, one that has a high sensitivity to changes in the radiative forcing and one that has a low sensitivity (these three are labelled '-ref', '-high' and '-low' in the following).

Change with time of the radiative forcing in RCA3 is prescribed to follow the emission scenario as in the driving global model. As RCA3 does not explicitly account for different greenhouse gases and/or aerosols this is accomplished for by changing the equivalent CO_2 concentration that is calculated according to IPCC (2001, table 6.2.1)

$$\Delta F = 5.35 \ln (CO_2/CO_{2ref}), \quad (1)$$

where ΔF is the radiative forcing and CO_{2ref} is the concentration in 1990. The radiative forcing for the emission scenarios is taken from IPCC (2001, table II.3.11). For further details of the application of the forcing conditions in the experiments described later see Kjellström et al. (2005) and Persson et al. (2007).

2.4. Method of comparing data sets

We calculate seasonal averages for the nominal seasons winter (December, January and February, hereafter DJF), spring (MAM), summer (JJA) and fall (SON). In addition we also calculate annual averages (ANN). These averages are calculated for each year in 30-yr periods both for the control period (1961–1990) and for three future time periods (2011–2040, 2041–2070 and 2071–2100). Five hundred bootstrap samples of the seasonal and annual means are generated to determine the statistical significance for the climate change signal for different periods and for differences between the simulated and observed climate for the control period. From these 500 bootstrap samples we collect statistics for each individual simulation in Table 1 and for the ensemble mean and estimate the differences that are significant at the 5% significance level.

3. Results and discussion

3.1. Simulated control climate (1961–1990)

3.1.1. Reanalysis-driven simulation.. Given perfect boundary conditions from ERA40 RCA3 simulates seasonal mean features of the circulation patterns (i.e. MSLP) very close to ERA40 itself (Figs. 1 and 2). The only exception is that MSLP over the western Mediterranean Sea is slightly too high in winter indicating that the cyclonic activity in this region is suppressed (Fig. 1). The good performance in simulating the large-scale circulation is a prerequisite for a good simulation also of other aspects of climate. In terms of T_{2m} the simulated climate is in relatively good agreement with the observed climate (Samuelsson et al., 2011). For seasonal mean T_{2m} this means that differences are mostly smaller than 2 °C although statistically significant differences of more than 3–4 °C exist in parts of the model domain in winter, which is the season showing the largest biases (Fig. 1). In summer only small areas with statistically significant biases

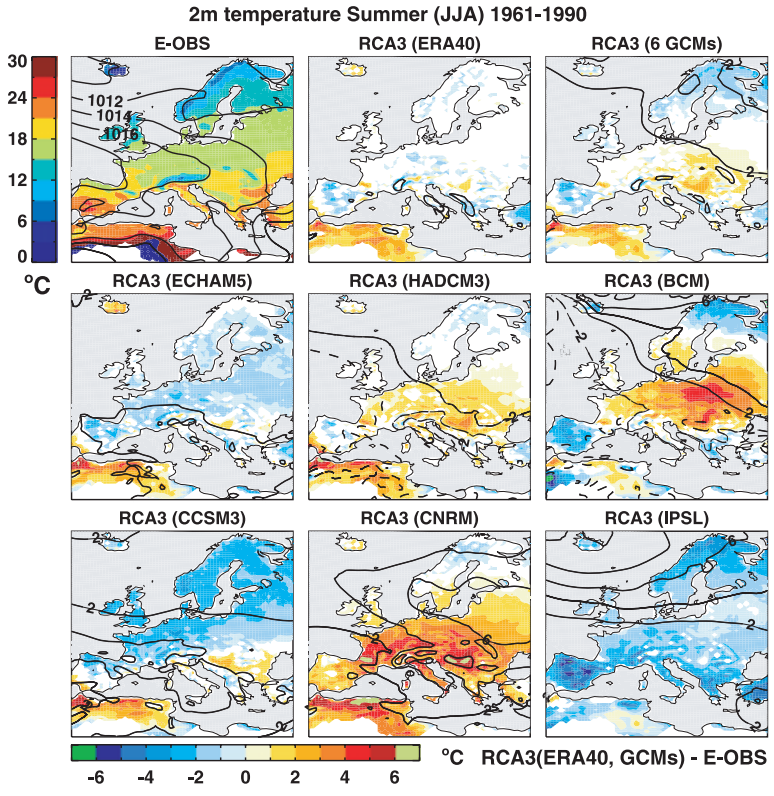

Fig. 2. (top, left-hand panel) Summer (JJA) mean T_{2m} (colour, °C, E-OBS) and MSLP (hPa, ERA40) and biases of T_{2m} and MSLP in the RCA3 simulations driven by (top, middle panel) the ERA40 reanalysis, (middle and bottom rows) six different GCMs and (top, right-hand panel) their ensemble mean. Only T_{2m} differences significant at the 5% significance level are shown. Correspondingly, statistically significant differences for MSLP are indicated with thick lines.

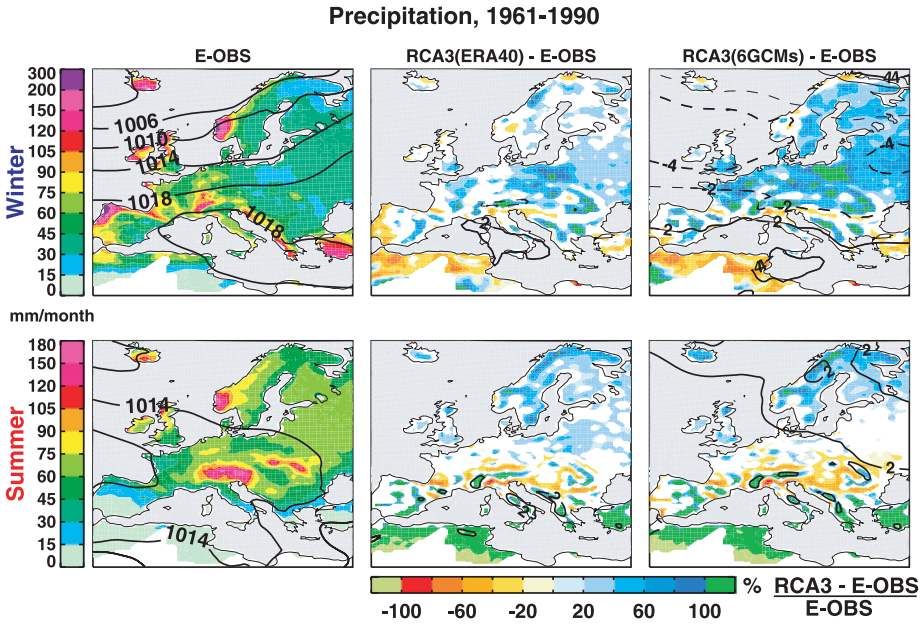

Fig. 3. (Upper row) winter (DJF) and (lower) summer (JJA) conditions for (left-hand panel) mean P (colour, mm per month, E-OBS) and MSLP (hPa, ERA40) and biases of P (%) and MSLP estimated from the RCA3 simulations driven by (middle panel) the ERA40 reanalysis and (right-hand panel) the mean of the six-member A1B-ensemble, with respect to the E-OBS and ERA40 (1961–1990). Only P differences significant at the 5% significance level are shown. Correspondingly, statistically significant differences for MSLP are indicated with thick lines.

exists, mostly in the Mediterranean region (Fig. 2). As further discussed in Samuelsson et al. (2011) and Nikulin et al. (2011) biases in T_{2m} in forested areas are reduced if comparison is made between the simulated T_{2m} for the open land fraction of the grid boxes instead of grid box averages as is done here. The open land fraction T_{2m} is more representative of what is observed at the observational stations that are generally located in open land areas.

Compared to the E-OBS data set P in RCA3 (ERA40) is overestimated in a large fraction of the model domain during winter while the overestimation is restricted more to the northern parts during summer (Fig. 3). In central and southern Europe both areas of over- and underestimation are seen in summer. These areas are partly colocated with high-altitude areas as RCA3 tends to give more P than observed over the mountain ranges and less in adjacent low-altitude regions (see for instance the Alps and the Pyrenees). Local and regional biases of up to or over 100% exist in northern Scandinavia, particularly in spring (not shown). In a previous study, however, Lind and Kjellström (2009) show that the present RCA3 simulation forced by ERA40 on the lateral boundaries gives a good correspondence to a high-resolution bias-corrected gridded data set for P in the Baltic Sea drainage basin during 1995–2000 and that annual mean net P (precipitation minus evaporation) over land agrees well with observed discharge for this region. Further they showed that large differences between different observational climatologies preclude any firm conclusions on the quality of the simulated water budget in that area.

3.1.2. GCM-driven simulations. In the GCM-forced simulations biases in T_{2m} and P are generally larger than in RCA3 (ERA40). This is to a large degree related to errors in how the GCMs simulate aspects of the general circulation. The relation between large-scale circulation and biases in temperature and precipitation climate is discussed for a range of GCMs, including some used here, by van Ulden and van Oldenburgh (2006). As a measure of the agreement between simulated and ERA40 MSLP they use the explained variance (E) that is defined as

$$E = 1 - \frac{\sigma^2_{\text{diff}}}{\sigma^2_{\text{obs}}}. \quad (2)$$

Here, σ^2 is the variance in space of (i) the difference between simulated and observed long-term average MSLP and (ii) the observed long-term average MSLP, respectively. E is close to 1 if the spatial variance in the difference field is small compared to the spatial variance in the observations. This implies that E close to 1 means a good agreement to observations both in terms of amplitude and gradients while low or negative numbers implies a poor agreement. We derive E by calculating 30-yr averages for each 3-month season in the RCA3 (GCM)-simulated MSLP compared to the corresponding ERA40 MSLP for 1961–1990. As the large-scale circulation in RCA3 is to a large degree dependent on the forcing GCM our calculated E is more to be considered as a test of how well the GCM simulates the large-scale circulation for the European region than a test of RCA3 itself. As a comparison, the RCA3 (ERA40) simulation yields an E that is above 0.96 for all seasons indicating a very

Table 2. Performance in the 1961–1990 period for the RCA3 (GCM) simulations

Forcing GCM	Large-scale circulation (E)				Temperature (MAE, °C)				Precipitation (MAE, %)			
	DJF	MAM	JJA	SON	DJF	MAM	JJA	SON	DJF	MAM	JJA	SON
ERA40	0.98	0.97	0.96	0.98	1.23	0.78	0.60	0.92	29.2	40.2	41.3	28.2
CNRM	*0.83*	*0.77*	*0.41*	*0.91*	*1.70*	*1.36*	*2.34*	*1.16*	*47.4*	*50.4*	*45.2*	*30.4*
BCM	*0.48*	*−0.80*	*−1.13*	*0.46*	*2.18*	*1.57*	*1.83*	*1.44*	*57.2*	*60.2*	*94.3*	*50.1*
CCSM3	*−0.35*	*−5.38*	*0.33*	*0.63*	*2.71*	*0.87*	*1.76*	*1.00*	*60.2*	*65.4*	*41.7*	*37.8*
ECHAM5-r1	0.86	0.64	0.66	0.93	2.00	1.07	1.00	0.93	46.8	47.7	40.6	43.7
ECHAM5-r2	0.83	0.55	0.68	0.93	1.64	0.80	1.02	1.02	46.9	48.0	39.1	44.2
ECHAM5-r3	*0.86*	*0.28*	*0.63*	*0.92*	*2.01*	*0.90*	*1.05*	*0.92*	*45.9*	*50.8*	*38.9*	*42.6*
HadCM3-ref	*0.86*	*−0.25*	*0.55*	*0.62*	*1.12*	*0.87*	*1.01*	*0.72*	*46.0*	*55.0*	*45.7*	*36.2*
HadCM3-low	0.66	−0.40	0.44	0.67	2.08	1.29	1.41	1.69	41.0	52.0	61.2	32.6
HadCM3-high	0.81	0.82	0.61	0.83	1.64	1.02	1.98	1.03	55.3	55.9	62.4	37.1
IPSL	*0.58*	*−1.08*	*−0.55*	*0.77*	*2.13*	*2.24*	*1.95*	*2.31*	*33.9*	*39.7*	*81.3*	*39.3*
Ensemble mean	*0.71*	*0.44*	*0.79*	*0.91*	*1.38*	*0.86*	*0.92*	*0.75*	*49.5*	*55.1*	*48.5*	*38.6*

Notes: The large-scale circulation is tested by the explained variance of mean sea level pressure (E, see text for description). For temperature and precipitation the mean absolute error (MAE) is calculated by averaging all local biases over the land areas within the domain restricted by (10.5°W–30°E, 36°N–70°N). The ensemble mean is calculated for the six simulations in italics.

good agreement to the large-scale circulation features imposed on the boundaries. For the GCM-forced runs the agreement is worse and some models even show negative numbers (Table 2). Best performance is seen for RCA3 (CNRM, ECHAM5-*r*3, HadCM3-ref and HadCM3-low). For RCA3 (IPSL, BCM and CCSM3) the agreement is worse with low or sometimes even negative E. The agreement is generally best in fall and winter and in most models worst in spring or summer. The poor agreement in spring/summer is a result of the fact that the observed spatial variability (σ^2_{obs}) is low in these seasons, unnormalized differences (σ^2_{diff}) are larger during fall/winter. Also the ensemble mean shows a good reproduction of the large-scale circulation although slightly worse than the best ensemble members. This relatively good agreement between the ensemble mean and ERA40 indicates that the averaging leads to a cancellation of some of the errors seen in simulations downscaling single GCMs.

The index E integrates over the area but does not reveal geographical details in the bias pattern, this can instead be inferred from maps. In winter for example, all simulations are too zonal in varying degree in parts of the North Atlantic and European region (Fig. 1). As a result of the errors in the wintertime circulation patterns too much mild and moist air is advected from the North Atlantic in over Europe. Therefore, both DJF $T_{2\mathrm{m}}$ (Fig. 1) and P (Fig. 3) are overestimated over large parts of the continent in these simulations. This overestimation is most pronounced in RCA3 (CCSM3) that also has the largest deviations in MSLP for this season. An exception to this general feature is the RCA3 (IPSL) simulation that is too cold and also drier (not shown) than the others despite the fact that also IPSL is too zonal in the South. The reason for the low temperatures in this simulation is not entirely clear but it can be seen that IPSL is too cold in large parts of the Northern Hemisphere mid-latitudes (Randall et al., 2007). Among the other models it is worthwhile mentioning that the large-scale circulation pattern in HadCM3-ref is in relatively good agreement with ERA40 (E-value of 0.86) even if MSLP in central Europe is too low indicating too much cyclonic activity in this area. For this particular model downscaling with RCA3 yields a temperature climate that is in good agreement to the observed climate (Fig. 1) while P in central Europe is overestimated (not shown). Apart from different large-scale circulation in the GCMs also differences in SST and sea-ice conditions lead to differences in the simulated regional climate. In the far North this sometimes leads to large cold biases of more than 6 °C as for the Icelandic region in RCA3 (HadCM3-ref, IPSL) and for northernmost Scandinavia in RCA3 (IPSL, BCM and CNRM).

Also during summer some large differences exist (Figs. 2 and 3). In RCA3 (ECHAM5-*r*3, CCSM3 and IPSL) the climate is generally too cold and too wet (not shown) in the North. In RCA3 (ECHAM5-*r*3 and CCSM3) this seems to be related to a too zonal circulation implying exaggerated transport of cool and moist air from the North Atlantic in over the European continent. In RCA3 (IPSL) this is not the case as that particular simulation is less zonal than the ERA40 MSLP pattern indicates. For the other three GCMs the downscaled summertime climate is too warm in most of continental Europe. The very different biases in summer time $T_{2\mathrm{m}}$ in these three simulations compared to the other three are related to the hydrological cycle. This can be illustrated by comparing RCA3 (CCSM3) that is too cold and RCA3 (CNRM) that is too warm in summer. In spring, P in much of western and central Europe is overestimated in RCA3 (CCSM3) while it is underestimated in RCA3 (CNRM) (not shown). As a consequence, the soils dries out more readily in summer in RCA3 (CNRM) allowing $T_{2\mathrm{m}}$ to increase while latent heat release from the wetter soils in RCA3 (CCSM3) moderates temperature increase in these areas. Similarly, differences in springtime P between RCA3 (CCSM3) and RCA3

(ECHAM5-*r*3) may also explain why summertime T_{2m} in the latter is in better agreement with observations despite the fact that ECHAM5 is too zonal.

The three RCA3 (ECHAM5) simulations are close to each other in terms of the 30-yr averages discussed here (Table 2). Also a closer inspection of those three simulations shows that all have too zonal conditions both in summer and winter leading to common bias patterns in temperature and *P* (not shown). The three RCA3 (HadCM3) simulations on the other hand, are much more distant from each other. The numbers in Table 2 partly shows this but as they represent mean average errors they do not give the full picture. In this case RCA3 (HadCM3-low) has relatively large negative biases in temperature while RCA3 (HadCM3-high) has warm biases (not shown). RCA3 (HadCM3-high) is too dry in parts of southern Europe while RCA3 (HadCM3-low) tends to be too wet. Of the three simulations forced by HadCM3 RCA3 (HadCM3-ref) is clearly the one showing the smallest biases. The differences between the three RCA3 (HadCM3) simulations are as large as differences between RCA3 simulations driven by other GCMs.

Summarized for the European continent local biases in temperature are up to 3–4 °C and up to 100% in *P* or even more in some of the simulations. Taken as area averages over the continent mean absolute errors in the simulations are in general 1–2 °C and 30–60%, respectively (Table 2). For most GCM-driven simulations the biases are larger than the corresponding errors in RCA3 (ERA40). The *P* biases are smallest in fall and winter that are also the seasons for which most simulations show the best correspondence to the large-scale circulation. For temperature, the biases are smallest in the transition seasons and larger in winter and summer. The six-member ensemble mean shows a better correspondence to observed temperature than most individual simulations it is based on for all seasons. This is caused by the fact that biases of opposite signs in the models tend to cancel each other when added, cf. RCA3 (CCSM3 and IPSL) in Fig. 1. For *P* this is not the case as the biases are more systematic with overestimated *P* in the North and a mixture of over- and underestimated *P* in the South regardless of forcing GCM. Therefore, the ensemble means bias is not smaller than many of the biases in the individual simulations underlying it.

3.2. *Simulated climate change*

3.2.1. Temperature climate. The simulated DJF circulation patterns are changing between 1961–1990 and 2071–2100. Five out of the six models show increasing MSLP in parts of southern Europe and the Mediterranean area indicating lower cyclonic activity in this region (Fig. 4) and a more zonal flow over central and northern Europe. Lower cyclonic activity in the Mediterranean area is in accordance to results presented by Pinto et al. (2007) for the ECHAM5 model. They show that this model has a lower cyclone track density in this area by the end of the century. The above-mentioned changes in circulation contributes to the large increase in T_{2m} in northern Europe as seen in Fig. 4. The largest temperature increases are found in the northeastern part of the domain, most notably in northern Fennoscandia, the Kola Peninsula and the ocean areas close to the northern rim. But, as this is the area of maximum warming also in the simulation not showing increasing MSLP in southern Europe RCA3 (HadCM3-ref) the contribution from changing large-scale circulation is not the major explanation of the large warming in this area. Instead positive feedback processes related to the retreat of the snow

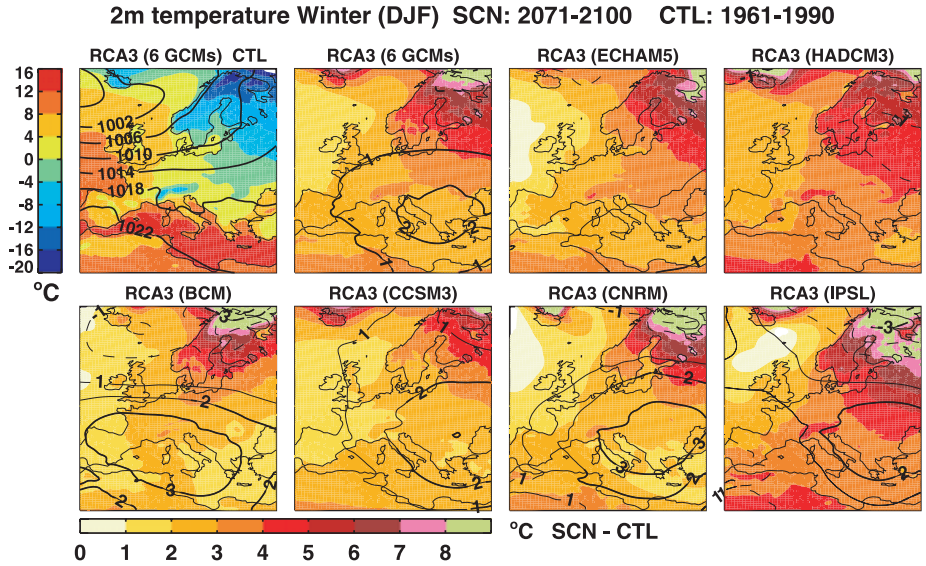

Fig. 4. The ensemble mean of winter (DJF) T_{2m} and MSLP for 1961–1990 (top left-hand panel) and the respective changes of T_{2m} and MSLP in 2071–2100 relative to 1961–1990 for the ensemble mean and the individual runs forced by A1B. Units are °C and hPa. Only T_{2m} differences significant at the 5% significance level are shown. Correspondingly, statistically significant differences for MSLP are indicated with thick lines.

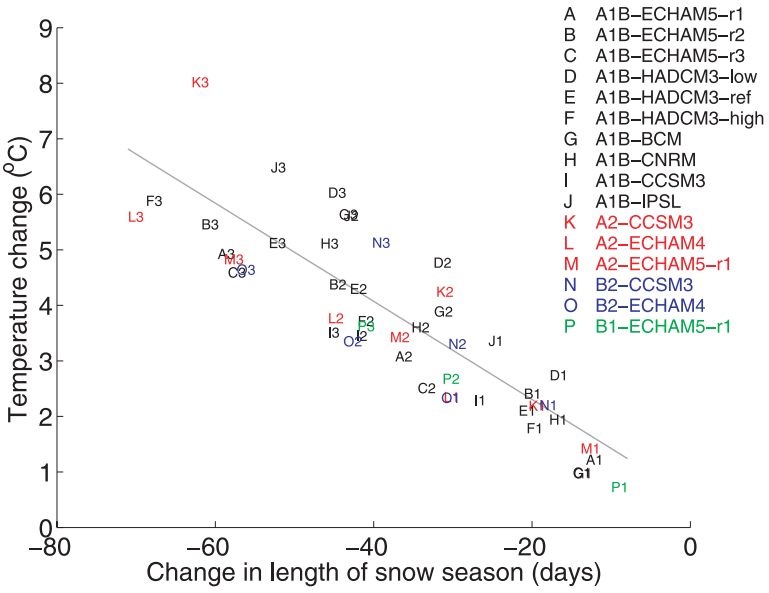

Fig. 5. Change in winter (DJF) T_{2m} (°C) versus change in the number of days with snow cover as an average over all land areas in the Scandinavian region (55–70°N, 4.5–30°E). Emission scenarios and forcing GCMs for each RCA3-simulation are given in the legend (A–P). Simulated changes are shown for three different time periods; (1) 2011–2040, (2) 2041–2070 and (3) 2071–2100. The grey line is a least-square fit to the data (the slope k is –0.09 d per °C and the correlation coefficient r is –0.87).

cover (Chapin et al., 2005) and the strong reduction in Arctic sea-ice (Perovich et al., 2007) are expected to play a role here. There is indeed a strong connection between decreasing snow cover and increasing temperature in this region in all simulations as exemplified for the Scandinavian region in Fig. 5. However, it is difficult to judge if this strong increase in temperature is a result or a cause of the decreasing snow cover. By comparing data from the three time periods the gradual decrease in snow cover as temperature increases over time is clearly seen for this region in all 16 simulations. Corresponding to the large change in the northeast, local maxima in warming are seen in the Alpine region that also face a major retreat in snow cover (Fig. 4).

We note that the three ECHAM5-A1B driven simulations show very different response in some of the time periods for the Scandinavian area (Fig. 5). In the time period 2011–2040 one of them, RCA3 (ECHAM5-*r*2) shows a warming that is more than 1.5 °C higher than in RCA3 (ECHAM5-*r*3). This is purely a result of natural variability and can to a large degree be explained by differences in large-scale circulation in the simulations. In this case the RCA3 (ECHAM5-*r*2) gives an increase in the North–South pressure gradient over the North Atlantic leading to mild conditions in northern Europe (not shown). Such differences in the climate change signal in the three ECHAM5-A1B driven simulations are seen also for other periods throughout the simulation with a maximum difference for the Scandinavian area of about 1.7 °C (Fig. 6). For similar reasons of changing large-scale circulation, RCA3 (HadCM3-low) shows a larger warming in much of Europe than RCA3 (HadCM3-high) for 2011–2040. This is despite the fact that global warming in HadCM3-high is larger than that in HadCM3-low for this time period. Interestingly RCA3 (HadCM3-low) shows a larger warming than RCA3 (HadCM3-high) for the Scandinavian region during the whole scenario period (Fig. 6). This is related to

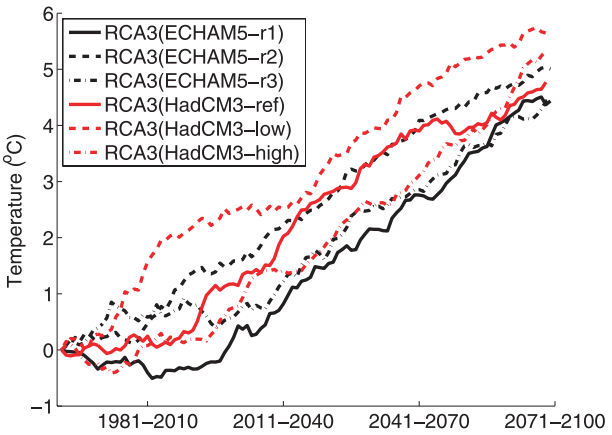

Fig. 6. Thirty-year running mean winter (DJF) T_{2m} anomalies w.r.t. the 1961–1990 average for all land in the Scandinavian region (55–70°N, 4.5–30°E). Results are shown for the simulations driven by the three ECHAM5-A1B ensemble members and the three HadCM3 perturbed physics ensemble members.

cold conditions in the northern part of this relatively large area in the control period in RCA3 (HadCM3-low), in other parts of Europe RCA3 (HadCM3-high) shows a larger warming for most of the years. These examples clearly show that natural variability adds significantly to the total spread in the climate change signal and that the contribution can be as large as the spread due to choice of GCM and/or emission scenario at some time periods. In the nearest decades natural variability may even completely offset the climate change signal for some variables in parts of Europe.

Changes in the large-scale circulation in JJA are small as can be inferred from the fairly small changes in MSLP shown in Fig. 7. In three simulations RCA3 (BCM, CNRM and IPSL)

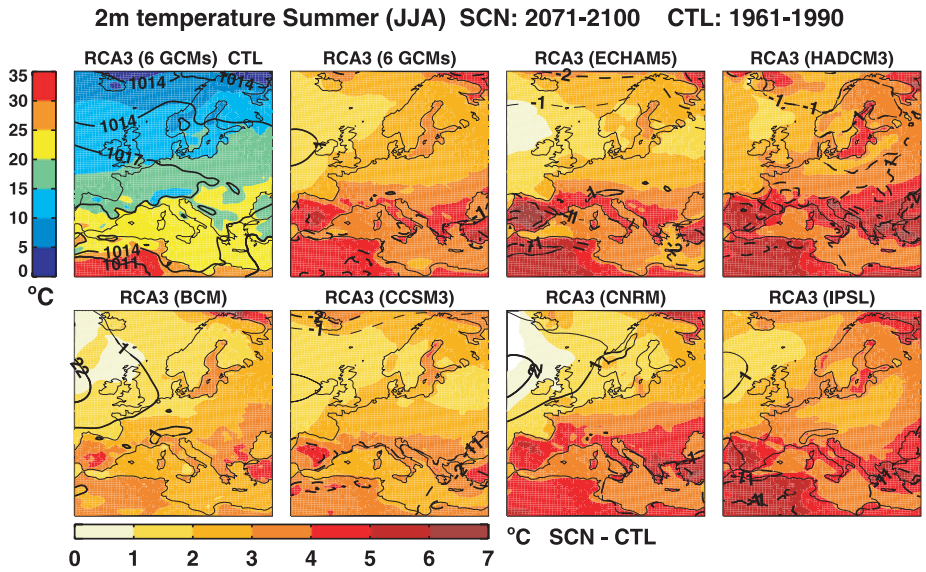

Fig. 7. The ensemble mean of summer (JJA) T_{2m} and MSLP for 1961–1990 (top left-hand panel) and the respective changes of T_{2m} and MSLP in 2071–2100 relative to 1961–1990 for the ensemble mean and the individual runs forced by A1B. Units are °C and hPa. Only T_{2m} differences significant at the 5% significance level are shown. Correspondingly, statistically significant differences for MSLP are indicated with thick lines.

there is an indication of a slightly stronger high pressure in the North Atlantic (cf. Fig. 4). These changes are smaller than the corresponding MSLP changes in DJF. Changes in T_{2m} are smaller over northern Europe and larger over the continent than in DJF. In summer it is southern Europe that generally experiences the largest changes with seasonal mean T_{2m} increasing by up to more than 6 °C in parts of the Iberian Peninsula in RCA3 (ECHAM5-r3). Regionally large changes are also seen over the ocean areas close to the northern boundary including the Barents Sea and the White Sea. Also the Baltic Sea is an area showing larger warming by 1–2 °C than surrounding land areas in all six simulations. These large changes in the northern ocean areas are related to the shortened season with sea-ice allowing for more heat being stored in the water as the heat required to melt the sea-ice decreases. Contrastingly, the air over the ice-free Mediterranean Sea warms less than that over the surrounding continents. Such a relatively smaller change over ocean compared to that over land is common also in GCMs as discussed for both transient and equilibrium climate change simulations by Manabe et al. (1991).

By the end of the century the forced temperature changes are larger than natural variability implying that they are statistically significant. All six simulations in Fig. 4 show statistically significant changes in all of the model domain except for RCA3 (CNRM) in which there is a small area of the north western model domain over the North Atlantic with non-significant changes. The changes in the other 10 simulations are also statistically significant in virtually all of the model domain by the end of the century for all seasons (not shown). Further, already at earlier time periods the temperature changes get statistically significant in large parts of the model domain. In the nearest decades (2011–2040) temperature changes are statistically significant in more than 70% of the model domain in most simulations in all seasons and by the mid of the century (2041–2070) the same holds true for more than 95% of the area.

3.2.2. Precipitation climate. Precipitation increases in northern and decreases in southern Europe in both winter and summer (Figs. 8 and 9). Differing between the seasons is the borderline between the areas of increase and decrease as this migrates from the North to the South and back again during the course of a year. The borderline is actually a relatively broad zone extending 500–1000 km or more in the North-South direction. An implication of this is that the P change in much of central Europe is uncertain not just in magnitude but also in sign in large parts of the year. This pattern of simulated P change including differences between seasons is in line with that in previous work on larger ensembles of regional climate scenarios derived directly from GCMs (e.g. Christensen et al., 2007). Increased zonality over parts of central and northern Europe during winter in RCA3 (BCM, CCSM3, CNRM, ECHAM5-r3 and IPSL) contributes to more P in this area. But, as large P increases are seen also in RCA3 (HadCM3-ref) that does not show any significant change in the large-scale circulation in winter, this can not be the only explanation and therefore also thermodynamic factors with more moisture in a future warmer atmosphere have to play a role as discussed in Christensen et al. (2007). A strong correlation between increasing temperature and P is indeed seen in northern Europe as exemplified for all land areas in the Scandinavian region in Fig. 10. The increase in P is 5.6% per °C local temperature increase and slightly more compared to the temperature increase upwind to Scandinavia over the North Atlantic. This increase in P is even larger than the average 4% per °C increase in

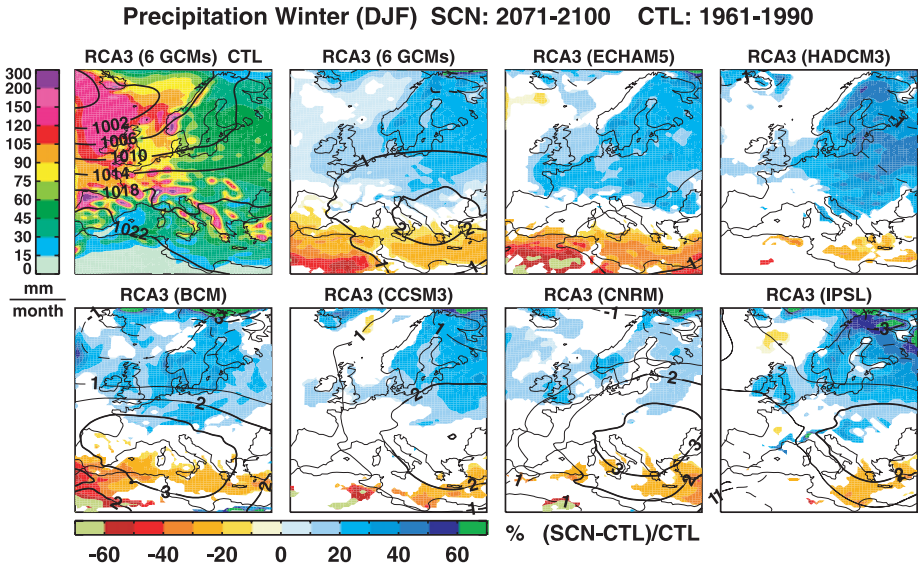

Fig. 8. The ensemble mean of winter (DJF) *P* (mm per month) and MSLP (hPa) for 1961–1990 (top left-hand panel) and the respective changes of *P* (%) and MSLP (hPa) in 2071–2100 relative to 1961–1990 for the ensemble mean and the individual runs forced by A1B. Only *P* differences significant at the 5% significance level are shown. Correspondingly, statistically significant differences for MSLP are indicated with thick lines.

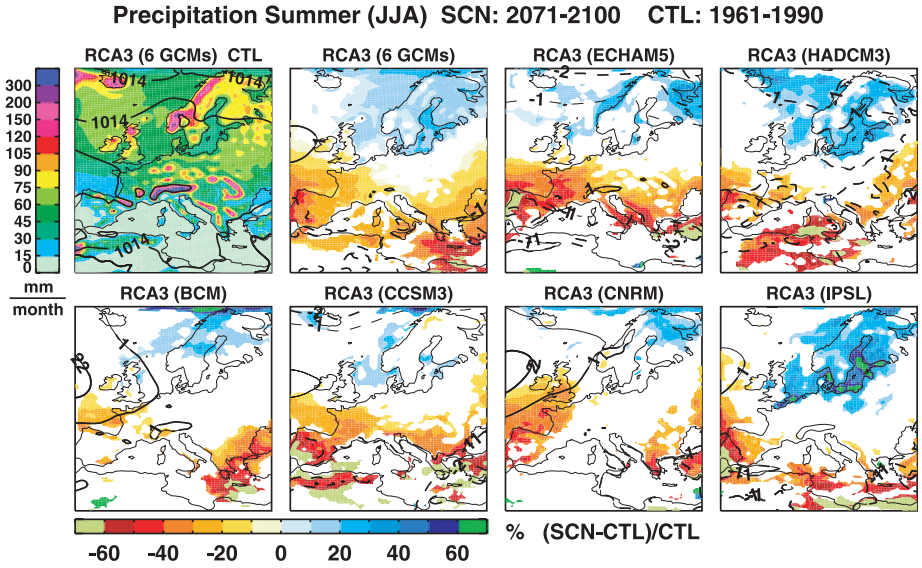

Fig. 9. The ensemble mean of summer (JJA) *P* (mm per month) and MSLP (hPa) for 1961–1990 (top left-hand panel) and the respective changes of *P* (%) and MSLP (hPa) in 2071–2100 relative to 1961–1990 for the ensemble mean and the individual runs forced by A1B. Only *P* differences significant at the 5% significance level are shown. Correspondingly, statistically significant differences for MSLP are indicated with thick lines.

poleward moisture transport reported by Held and Soden (2006) for mid-latitudes where the increase has its maximum. This indicates a local amplification of the hydrological cycle in northern Europe as earlier discussed for the Baltic Sea drainage basin for three of the present simulations, RCA3 (ECHAM4-A2/B2 and ECHAM5-r1-A1B) by Kjellström and Lind (2009). In some simulations part of this amplification seems to be related to the Baltic Sea as significant increases in summertime *P* is seen over the Baltic Sea in RCA3 (HadCM3-ref and IPSL). These are also the two simulations showing the largest increase in T_{2m} in that region. This strong relation between *P* and SST indicates a sensitivity to change in SSTs in this area as earlier shown for a range of RCMs in the PRUDENCE project (Kjellström and Ruosteenoja, 2007).

The geographical details of the change in *P* differ between the different simulations but the major features including the increase in the North and the decrease in the South together with the seasonal migration of the border zone are represented

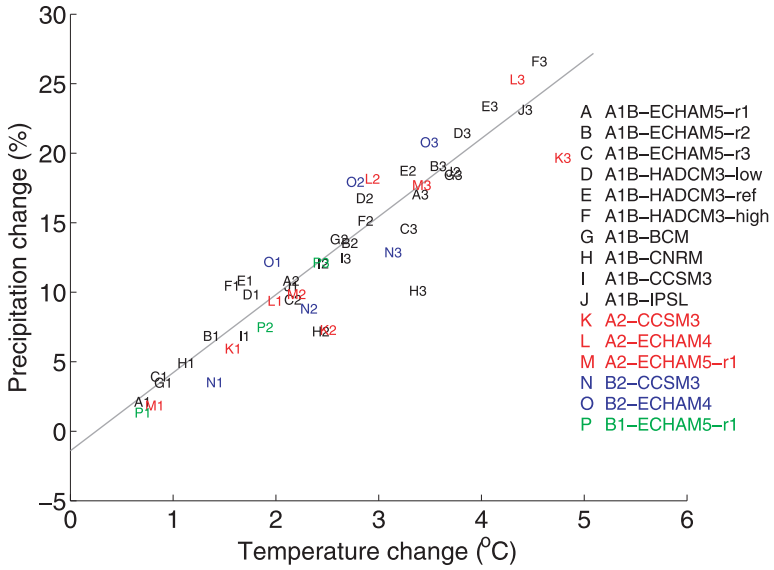

Fig. 10. Change in ANN P (%) versus T_{2m} (°C) over all land in the Scandinavian region (55–70°N, 4.5–30°E). Emission scenarios and forcing AOGCM for each RCA3-simulation are given in the legend (A–P). Simulated changes are shown for three different time periods; (1) 2011–2040, (2) 2041–2070 and (3) 2071–2100. The grey line is a least-square fit to the data (the slope k is 5.6% per °C and the correlation coefficient r is 0.93).

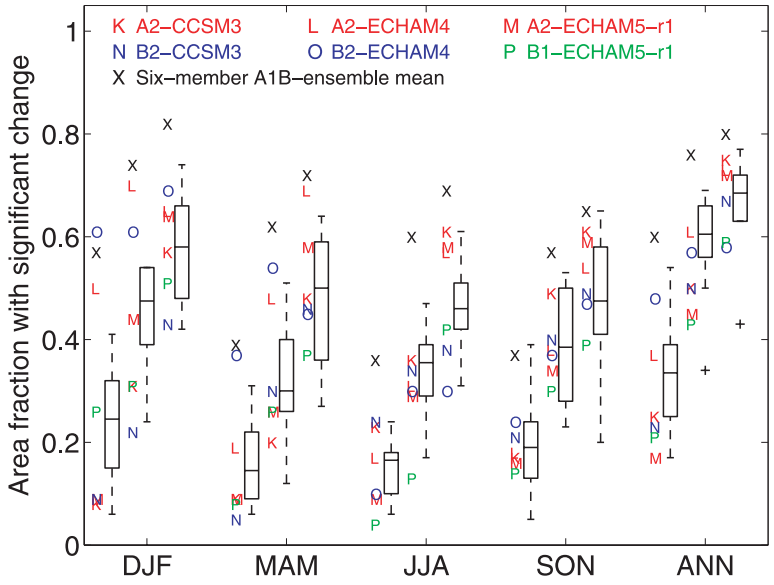

Fig. 11. Fraction of area where the change in P is statistically significant at three different time periods; 2011–2040 (left-hand panel), 2041–2070 (middle panel) and 2071–2100 (right-hand panel) for the four seasons and the annual mean. The box and whisker plot shows the ten A1B scenarios. The horizontal bars in the boxes are lower and upper quartiles and the median, respectively. The whiskers extend from the box out to the most extreme data value within 1.5 times the interquartile range, outliers are denoted by (+). To the left of each box and whisker plot are shown the simulations with other emission scenarios and the six member A1B-ensemble mean.

in all simulations. The signal is more robust when calculated as an average over several simulations compared to looking at single simulations. This can be exemplified by the six-member A1B ensemble for which the fraction of the European continent where changes are statistically significant amounts to about 80% on an annual basis in the latter part of the century while single members give 45–75% (Fig. 11). It is also clearly seen that the statistical significance increases gradually with time and that the changes are most significant in winter. Further it can be noted that all A2-simulations (marked by red symbols) tend to cluster on the relatively more significant side in the last 30-yr period. This is not the case at the earlier two periods when the A2-simulations are spread out also at the low-end range and when A2-simulations sometimes show less change than corresponding B2-simulations. Therefore, the result suggests sensitivity to the emission scenario but not until the latter part of the century as presented for changes in global mean temperature (Meehl et al., 2007).

3.2.3. Wind climate. Changes in the wind climate differ more between the simulations than changes in other variables. A common feature is decreasing wind speed during winter in the Mediterranean area in most simulations (Fig. 12). These decreases in the wind speed are likely related to changes in the large-scale circulation as the Mediterranean area is projected to have less cyclonic influence and more anticyclonic conditions in the future. Several simulations show decreasing wind speed in the area of the Icelandic Low [RCA3 (ECHAM5-r3, IPSL and HadCM3-ref)] and in most of the Atlantic [RCA3 (IPSL)].

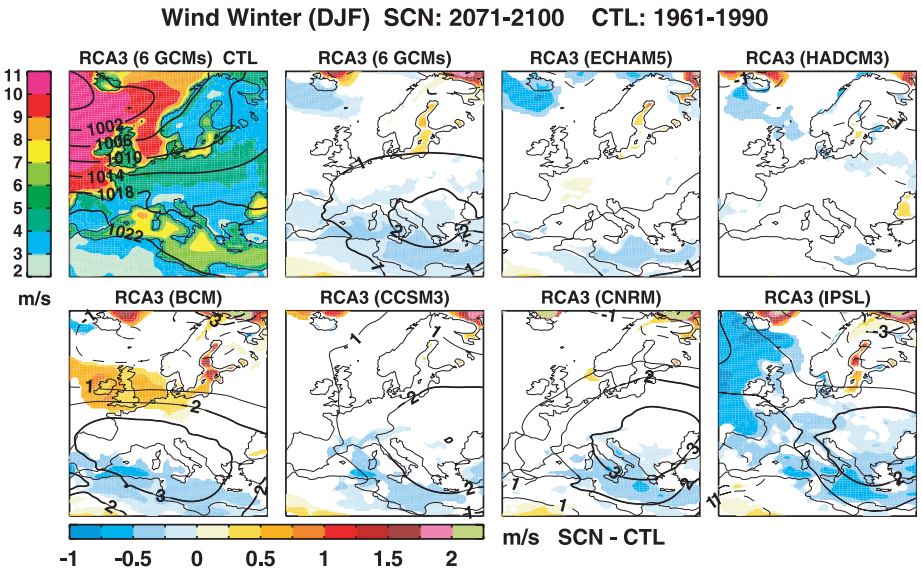

Fig. 12. (top left-hand panel) The ensemble mean of winter (DJF) mean W_{10m} and MSLP for 1961–1990 (top left-hand panel) and the respective changes of W_{10m} and MSLP in 2071–2100 relative to 1961–1990 for (top row, second from left-hand side) the ensemble mean and (top and bottom rows) the individual runs forced by A1B. Units are m s^{-1} and hPa. Only W_{10m} differences significant at the 5% significance level are shown. Correspondingly, statistically significant differences for MSLP are indicated with thick lines.

RCA3 (BCM) also shows a tendency of decreasing wind speed South of Iceland but otherwise increases in a westeasterly band over the North Atlantic, the British Isles and the southern Baltic Sea. In this particular simulation the increase can be connected to a sharpening of the North–South pressure gradient. All simulations also show statistically significant increases in wind speed over more or less large parts of the Baltic Sea, the White Sea, parts of the Barents Sea and the North Atlantic North of Iceland. These areas are all projected to have substantial reductions in sea-ice in the GCMs (not shown). Such reductions lead to higher near-surface temperatures and thereby reduced static stability in the lower atmosphere. This is true for winter but also for other seasons as the temperature increase more in those areas than in the surrounding land areas (cf. summer conditions in Fig. 7). As a result of the reduced static stability wind speed at low levels increase in most of the models in these areas as seen in Figs. 12 and 13.

Also in summer there is a tendency for decreasing seasonal mean wind speed in large parts of the model domain including the North Atlantic (Fig. 13). In the Mediterranean area, on the other hand, there are areas with increased wind speeds in many of the simulations. This may be connected to changing temperature conditions as the differential warming over sea and land leads to larger horizontal temperature gradients in parts of the Mediterranean region as the sea warms less than surrounding land areas (Fig. 7). Stronger temperature gradients in turn may lead to stronger thermally driven circulations and thereby higher wind speeds in some areas.

Although there are some coherent patterns in the change of wind speed in the simulations the climate change signal is much less robust than that for temperature and somewhat weaker than that for P. The total area projected to meet changes in the wind climate amounts to almost 80% for the six-member A1B ensemble mean (Fig. 14). As for P there is a gradual increase over time and also differences between seasons with the largest degree of statistical significance in summer by the end of the century. A difference compared to P is that the emission scenario does not seem to play such an important role. Here, changes in wind speed seem to be equally large in the A1B-simulations as in the A2-simulations. Instead choice of driving GCM seems to be more important in terms of change in the wind climate. This can be seen as the A2- and B2-simulations with RCA3 (ECHAM4) tend to cluster as well as do A2- and B1-simulations with RCA3 (ECHAM5) also at later time periods when the difference in emission scenarios plays an important role for P (Fig. 11).

3.2.4. Transient climate change. Some of the examples given above show that the climate change signal grows and that the statistical significance gets larger with time in the simulations. Here, we note that also the patterns of change that are seen for the last decades of the century emerge already earlier in the simulations. This is shown for the six-member ensemble with different GCMs on the boundaries under the A1B emission scenario (Figs. 15 and 16). In both figures it can be seen that particularly the geographical pattern of change in T_{2m} is very similar in the different time windows including features like the relatively small warming of the North Atlantic and the excessive warming of the Baltic Sea in summer. But, also changes in MSLP, P and W_{10m} becomes apparent in the nearest few decades or at the mid of the century.

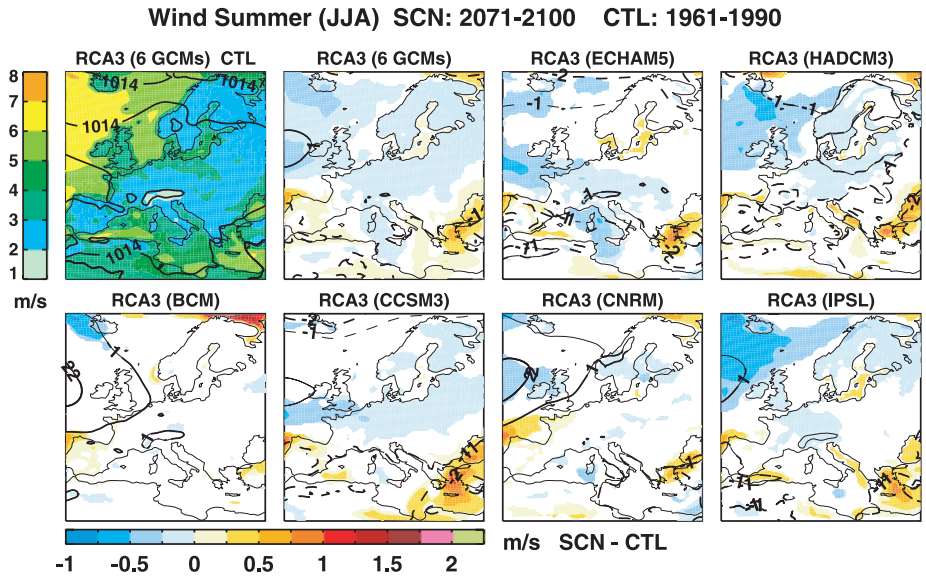

Fig. 13. (top left-hand panel) The ensemble mean of summer (JJA) mean W_{10m} and MSLP for 1961–1990 and the respective changes of W_{10m} and MSLP in 2071–2100 relative to 1961–1990 for (top row, second from left-hand side) the ensemble mean and (top and bottom rows) the individual runs forced by A1B. Units are ms^{-1} and hPa. Only W_{10m} differences significant at the 5% significance level are shown. Correspondingly, statistically significant differences for MSLP are indicated with thick lines.

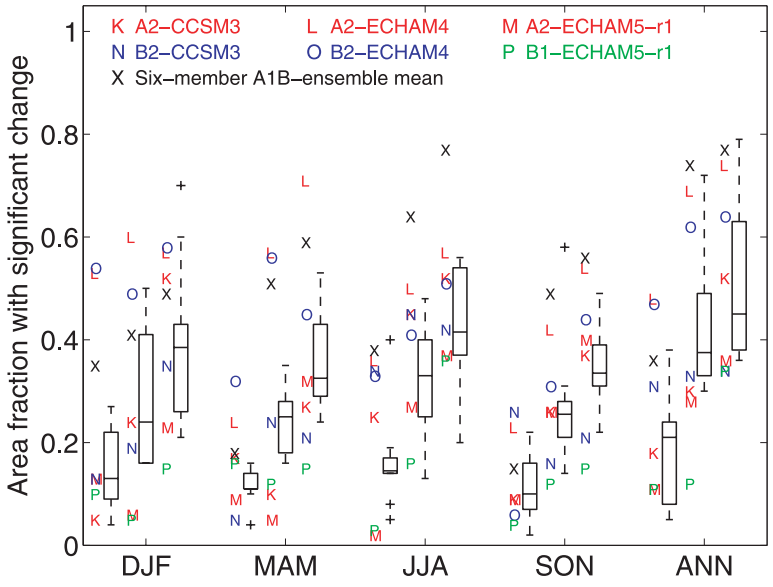

Fig. 14. Fraction of area where the change in W_{10m} is statistically significant at three different time periods; 2011–2040 (left-hand panel), 2041–2070 (middle panel) and 2071–2100 (right-hand panel) for the four seasons and the annual mean. The box and whisker plot shows the ten A1B scenarios. The horizontal bars in the boxes are lower and upper quartiles and the median, respectively. The whiskers extend from the box out to the most extreme data value within 1.5 times the interquartile range, outliers are denoted by (+). To the left of each box and whisker plot are shown the simulations with other emission scenarios and the six-member A1B-ensemble mean.

4. Summary and conclusions

In this study, we describe changes in seasonal mean features of T_{2m}, P and wind speed over Europe based on a 16-member ensemble of RCM simulations with the Rossby Centre regional atmospheric climate model RCA3. In the first part we describe characteristics of the simulated climate in 1961–1990 both when forced by reanalysis data and when forced by boundary data from GCMs. From this part of the study we find that:

(1) Biases in simulations of the recent past climate are larger when RCA3 has been forced by GCMs compared to when it has been forced by reanalysis data. Typical biases in the GCM-driven simulations are up to 3–4 °C for temperature and 100% for P.

(2) Biases are to a large degree related to errors in the representation of the large-scale circulation in the GCMs and to biases in SSTs and sea-ice cover in them.

(3) The ensemble mean is generally better than the individual simulations it consists of, at least for temperature but not necessarily for P.

In the second part of the paper we give an overview of the climate change signal in the ensemble by presenting seasonal

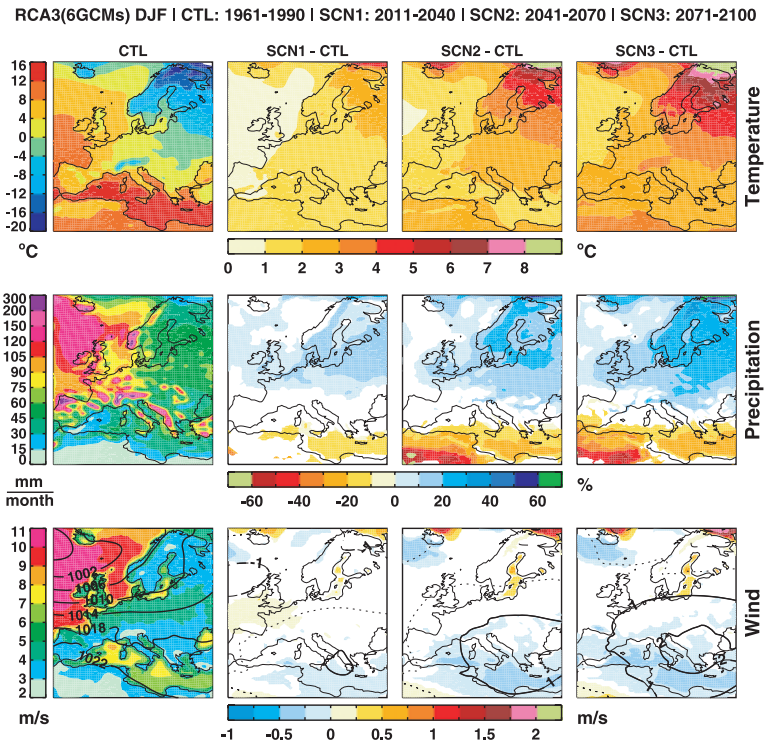

Fig. 15. Six-member A1B ensemble means of winter (DJF) T_{2m} (top panel), P (middle panel) and W_{10m} and MSLP (lower panel) for 1961–1990 (left column) and the respective changes in 2011–2040, 2041–2070 and 2071–2100 compared to 1961–1990 in the three rightmost columns. Only differences significant at the 5% significance level are shown. For MSLP all changes are shown but statistically significant differences are indicated with thick lines.

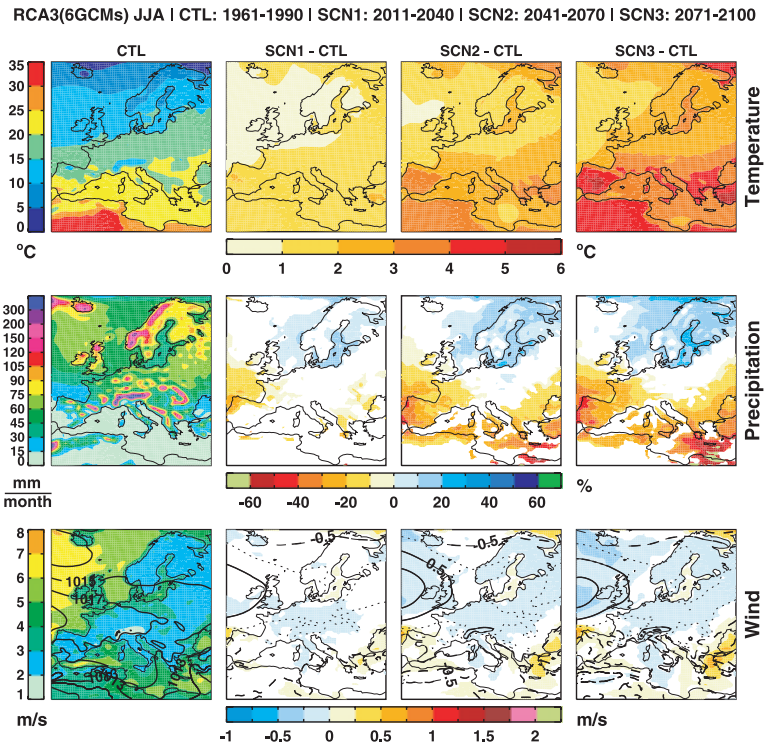

Fig. 16. Six-member A1B ensemble means of summer (JJA) T_{2m} (top panel), P (middle panel) and W_{10m} and MSLP (lower panel) for 1961–1990 (left column) and the respective changes in 2011–2040, 2041–2070 and 2071–2100 compared to 1961–1990 in the three rightmost columns. Only differences significant at the 5% significance level are shown. For MSLP all changes are shown but statistically significant differences are indicated with thick lines.

means of the mentioned variables including the spread between them as simulated in the different ensemble members. In general the results show statistically significant warming of the European continent in the future. This warming is most pronounced in the northeast during winter and in the South during summer. For P the signal is weaker but shows some distinct features as a general increase in the North and a decrease in the South. The borderline between increase and decrease is a fairly broad

(of the order of 500 km) zone that migrates back and forth from a northward position in summer to a southward position in winter. The projected change in the wind climate is statistically significant in a smaller fraction of the model domain compared to that in P indicating that future changes in wind speed are more uncertain. The main changes include generally decreasing winds in much of the model domain except for northern ocean areas during winter and for parts of the Mediterranean during summer where wind speed is projected to increase locally. From this part of the work we conclude:

(1) The spread in the results is largely dependent on the choice of GCMs. Further, the spread between them is to a great extent dependent on differences in changes of the large-scale circulation between the GCMs.

(2) Emission scenarios play an important role for the spread in temperature and P between ensemble members during the last decades of the century. At earlier periods it is not the dominating source of uncertainty. For wind speed the differences due to emission scenarios are smaller also at the end of the century.

(3) Natural variability is an important source of uncertainty for the next few decades sometimes clearly dominating over the spread due to model formulation (and thereby climate sensitivity).

(4) Ensemble means show tendencies for the next few decades in the direction of what the climate change scenarios show for the end of the century.

Finally we note that although this ensemble of 16 transient 140-yr simulations is unique as of today it still samples only a small part of the total uncertainty range. However, we have shown that such a small ensemble of climate change simulations may be useful in order to illustrate the uncertainties related to emissions, boundary conditions and natural variability in a physically consistent way at the regional scale. To fully explore the uncertainty ranges would require a much larger ensemble containing more forcing GCMs, emission scenarios and ensemble members sampling the natural variability. In addition also the uncertainty due to RCM formulation should be addressed. Therefore, the results presented here could be used together with other regional climate change matrices such as that developed in the ENSEMBLES project.

5. Acknowledgments

Part of the simulations and subsequent analysis work has been funded by the European ENSEMBLES (GOCE-CT-2003-505539) project, the Nordic Climate and Energy Systems project and the Swedish Mistra-SWECIA programme funded by Mistra (the Foundation for Strategic Environmental Research). The model simulations were made on the climate computing resource Tornado funded with a grant from the Knut and Alice Wallenberg foundation. The institutes providing the global model data used as boundary conditions are kindly acknowledged. We are grateful for the E-OBS data set from the EU-FP6 project ENSEMBLES (http://www.ensembles-eu.org) and the data providers in the ECA&D project (http://eca.knmi.nl). We acknowledge one of the anonymous reviewers for constructive comments that have been useful for improving the paper.

References

Barstad, I., Sorteberg, A., Flatøy, F. and Déqué, M. 2008. Precipitation, temperature and wind in Norway: dynamical downscaling of ERA40. *Clim. Dyn.* **33**, 769–776.

Beniston, M., Stephenson, D.B., Christensen, O. B., Ferro, C. A. T., Frei, C. and co-authors. 2007. Future extreme events in European climate: an exploration of regional climate model projections. *Clim. Change* **81**(Suppl.1), 71–95.

Bleck, R., Rooth, C., Dingming, H. and Smith L. T. 1992. Salinity-driven thermocline transients in a wind- and thermohaline-forced isopycnic Coordinate Model of the North Atlantic. *J. Phys. Oceanogr.* **22**, 1486–1505.

Chapin, F. S., III, Sturm, M., Serreze, M. C., McFadden, J. P., Key, J. R. and co-authors. 2005. Role of land-surface changes in Arctic summer warming. *Science* **310**, 657–660.

Christensen, J. H. and Christensen, O. B. 2007. A summary of the PRUDENCE model projections of changes in European climate by the end of the century. *Clim. Change* **81**(Suppl. 1), 7–30, doi:10.1007/s10584-006-9210-7.

Christensen, J. H., Hewitson, B., Busuioc, A., Chen, A., Gao, X. and co-authors. 2007. Regional Climate Projections. In: *Climate Change 2007: The Physical Science Basis. Contribution of Working Group I to the Fourth Assessment Report of the Intergovernmental Panel on Climate Change* (eds S. Solomon, D. Qin, M. Manning, Z. Chen, M. Marquis and co-editors). Cambridge University Press, Cambridge, UK and New York, NY, USA, 847–940.

Collins, W. D., Bitz, C. M., Blackmon, M. L., Bonan, G. B., Bretherton, C. S. and co-authors. 2006. The community climate system model version 3 (CCSM3). *J. Clim.* **19**, 2122–2143.

Collins, M., Booth, B. B., Bhaskaran, B., Harris, G. R., Murphy, J. M. and co-authors. 2010. Climate model errors, feedbacks and forcings: a comparison of perturbed physics and multi-model ensembles. *Clim. Dyn.* doi:10.1007/s00382-010-0808-0.

Déqué, M., Dreveton, C., Braun, A., and Cariolle, D. 1994. The ARPEGE/IFS atmosphere model. *Clim. Dyn.* **10**, 249–266.

Déqué, M., Rowell, D. P., Lüthi, D., Giorgi, F., Christensen, J. H. and co-authors. 2007. An intercomparison of regional climate simulations for Europe: assessing uncertainties in model projections. *Clim. Change* **81**(Suppl. 1), 53–70, doi:10007/s10584-006-9228-x.

Gibelin, A. L. and Déqué, M. 2003. Anthropogenic climate change over the Mediterranean region simulated by a global variable resolution model. *Clim. Dyn.* **20**, 327–339.

Gibson, J. K., Kållberg, P., Uppala, S., Hernandez, A., Nomura, A. and co-authors. 1997. *ERA Description, ERA-15 Project Report Series (ECMWF), No. 1*. ECMWF, Shinfield Park, Reading, United Kingdom.

Gordon, C., Cooper, C., Senior, C. A., Banks, H., Gregory, J. M. and co-authors. 2000. The simulation of SST, sea ice extents and ocean heat transports in a version of the Hadley Centre coupled model without flux adjustments. *Clim. Dyn.* **16**, 147–168.

Haugen, J. E. and Iversen, T. 2008. Response in extremes of daily precipitation and wind from a downscaled multimodel ensemble of anthropogenic global climate change scenarios. *Tellus* **60A**, 411–426.

Hawkins, E. and Sutton, R. 2009. The potential to narrow uncertainty in regional climate predictions. *Bull. Am. Meteorol. Soc.* **90**, 1095–1107, doi:10.1175/2009BAMS2607.1.

Haylock, M. R., Hofstra, N., Klein Tank, A. M. G., Klok, E. J., Jones, P. D. and co-authors. 2008. A European daily high-resolution gridded data set of surface temperature and precipitation for 1950–2006. *J. Geophys. Res.* **113**, D20119, doi:10.1029/2008JD010201.

Held, I. and Soden, B. 2006. Robust response of the hydrological cycle to global warming. *J. Clim.* **19**, 5686–5699.

Hewitt, C. and Griggs, D. 2004. Ensembles-based predictions of climate changes and their impacts. *EOS* **85**, 566, doi:10.1029/2004EO520005.

Hourdin, F., Musat, I., Bony, S., Braconnot, P., Codron, F. and co-authors. 2006. The LMDZ4 general circulation model: climate performance and sensitivity to parameterized physics with emphasis on tropical convection. *Clim. Dyn.* **27**, 787–813.

IPCC. 2001. Climate change 2001: the scientific basis. In: *Contribution of Working Group I to the Third Assessment Report of the Intergovernmental Panel on Climate Change* (eds J. T. Houghton, Y. Ding, D. J. Griggs, M. Noguer, P. J. van der Linden and co-editors). Cambridge University Press, Cambridge, UK, 881.

Jacob, D., Bärring, L., Christensen, O. B., Christensen, J. H., de Castro, M. and co-authors. 2007. An inter-comparison of regional climate models for Europe: design of the experiments and model performance. *Clim. Change* **81**(Suppl. 1), 31–52, doi:10007/s10584-006-9213-4.

Jones, C. G., Ullerstig, A., Willén, U. and Hansson, U. 2004. The Rossby Centre regional atmospheric climate model (RCA). Part I: model climatology and performance characteristics for present climate over Europe. *AMBIO* **33**, 199–210.

Jungclaus, J. H., Botzet, M., Haak, H., Keenlyside, N., Luo, J.-J. and co-authors. 2006. Ocean circulation and tropical variability in the coupled ECHAM5/MPI-OM. *J. Clim.* **19**, 3952–3972.

Kjellström, E. and Ruosteenoja, K. 2007. Present-day and future precipitation in the Baltic Sea region as simulated in a suite of regional climate models. *Clim. Change* **81**(Suppl. 1), 281–291.

Kjellström, E. and Lind, P. 2009. Changes in the water budget in the Baltic Sea drainage basin in future warmer climates as simulated by the regional climate model RCA3. *Boreal Environ. Res.* **14**, 114–124.

Kjellström, E., Bärring, L., Gollvik, S., Hansson, U., Jones, C. and co-authors. 2005. A 140-year simulation of European climate with the new version of the Rossby Centre regional atmospheric climate model (RCA3). In: *Reports Meteorology and Climatology*. Volume 108, SMHI, SE-60176 Norrköping, Sweden, 54.

Kjellström, E., Bärring, L., Jacob, D., Jones, R., Lenderink, G and co-authors. 2007. Modelling daily temperature extremes: recent climate and future changes over Europe. *Clim. Change* **81**(Suppl. 1), 249–265, doi:10007/s10584-006-9220-5.

Klok, E. J. and Klein Tank, A. M. 2008. Updated and extended European dataset of daily climate observations. *Int. J. Climatol.* **29**(8), 1182–1191.

Lind, P. and Kjellström, E. 2009. Water budget in the Baltic Sea drainage basin: evaluation of simulated fluxes in a regional climate model. *Boreal Environ. Res.* **14**, 56–67.

Ljungemyr, P., Gustafsson, N. and Omstedt, A. 1996. Parameterization of lake thermodynamics in a high resolution weather forecasting model. *Tellus* **48A**, 608–621.

Manabe, S., Stouffer, R. J., Spelman, M. J. and Bryan, K. 1991. Transient responses of a coupled ocean-atmosphere model to gradual changes of atmospheric CO_2. Part I: annual mean response. *J. Clim.* **4**, 785–818.

Meehl, G. A., Stocker, T. F., Collins, W. D., Friedlingstein, P., Gaye, A. T. and co-authors. 2007. Global climate projections. In: *Climate Change 2007: The Physical Science Basis. Contribution of Working Group I to the Fourth Assessment Report of the Intergovernmental Panel on Climate Change.* (eds S. Solomon and co-editors). Cambridge University Press, Cambridge, United Kingdom and New York, NY, USA.

Murphy, J. M., Booth, B. B. B., Collins, M., Harris, G. R., Sexton, D. M. H. and co-authors. 2007. A methodology for probabilistic predictions of regional climate change from perturbed physics ensembles. *Phil. Trans. R. Soc. A* **365**, 1993–2028.

Nakićenović, N. and Swart, R. Eds., 2000. Special report on emissions scenarios. In: *A Special Report of Working Group III of the Intergovernmental Panel on Climate Change*. Cambridge University Press, Cambridge, United Kingdom and New York, NY, USA, 599.

Nikulin, G., Kjellström, E., Hansson, U., Jones, C., Strandberg, G. and co-authors. 2011. Evaluation and future projections of temperature, precipitation and wind extremes over Europe in an ensemble of regional climate simulations. *Tellus* **63A**, 41–55.

Palmer, T. N., Alessandri, A., Andersen, U., Cantelaube, P., Davey, M. and co-authors. 2004. Development of a European multi-model ensemble system for seasonal to inter-annual prediction (DEMETER). *Bull. Am. Meteorol. Soc.* **85**, 853–872.

Perovich, D. K., Light, B., Eicken, H., Jones, K. F., Runciman, K. and co-authors. 2007. Increasing solar heating of the Arctic Ocean and adjacent seas, 1979–2005: attribution and role in the ice-albedo feedback. *Geophys. Res. Lett.* **34**, L19505, doi:10.1029/2007GL031480.

Persson, G., Bärring, L., Kjellström, E., Strandberg, G. and Rummukainen, M. 2007. Climate indices for vulnerability assessments. In: *Reports Meteorology and Climatology* Volume 111. SMHI, SE-60176 Norrköping, Sweden, 64.

Pinto, J. G., Ulbrich, U., Leckebusch, G. C., Spangehl, T., Reyers, M. and co-authors. 2007. Changes in storm track and cyclone activity in three SRES ensemble experiments with the ECHAM5/MPI-OM1 GCM. *Clim. Dyn.* **29**, 195–210, doi:10.1007/s00382-007-0230-4.

Räisänen, J., Hansson, U., Ullerstig, U., Döscher, R., Graham, L. P. and co-authors. 2004. European climate in the late 21st century: regional simulations with two driving global models and two forcing scenarios. *Clim. Dyn.* **22**, 13–31.

Randall, D. A., Wood, R. A., Bony, S., Colman, R., Fichefet, T. and co-authors. 2007. Climate models and their evaluation. In: *Climate Change 2007: The Physical Science Basis in Contribution of Working Group I to the Fourth Assessment Report of the Intergovernmental Panel on Climate Change* (eds S. Solomon, D. Qin, M. Manning, Z. Chen, M. Marquis and co-editors). Cambridge University Press, Cambridge, United Kingdom and New York, NY, USA.

Rockel, B. and Woth, K. 2007. Extremes of near-surface wind speed over Europe and their future changes as estimated from an ensemble of RCM simulations. *Clim. Change* **81**, 267–280.

Roeckner, E., Bengtsson, L., Feicther, J., Lelieveld, J. and Rodhe, H. 1999. Transient climate change simulations with a coupled atmosphere-ocean GCM including the tropospheric sulfur cycle. *J. Clim.* **12**, 3004–3032.

Roeckner, E., Brokopf, R., Esch, M., Giorgetta, M., Hagemann, S. and co-authors. 2006. Sensitivity of simulated climate to horizontal and vertical resolution in the ECHAM5 atmosphere model. *J. Clim.* **19**, 3771–3791.

Samuelsson, P., Gollvik, S. and Ullerstig, A. 2006. The Land-Surface Scheme of the Rossby Centre Regional Atmospheric Climate Model (RCA3). Report in Meteorology 122, SMHI. SE-601 76 Norrköping, Sweden, 25.

Samuelsson, P., Gollvik, S., Hansson, U., Jones, C., Kjellström, E. and co-authors. 2011. The rossby centre regional climate model RCA3: model description and performance. *Tellus*, **63A**, 4–23.

Sterl, A., Severijns, C., Dijkstra, H., Hazeleger, W., van Oldenborgh, G. J. and co-authors. 2008. When can we expect extremely high surface temperatures? *Geophys. Res. Lett.* **35**, L14703, doi:10.1029/2008GL034071.

Uppala, S. M., Kållberg, P. W., Simmons, A. J., Andrae, U., da Costa Bechtold, V. and co-authors. 2005. The ERA-40 Re-analysis. *Q. J. Roy. Meteorol. Soc.* **131**, 2961–3012.

Van Der Linden, P. and Mitchell, J. F. B. Eds., 2009. ENSEMBLES: Climate Change and Its Impacts: Summary of Research and Results From the ENSEMBLES Project. Met Office Hadley Centre, FitzRoy Road, Exeter EX1 3PB, UK, 160.

Van Ulden, A. P. and van Oldenborgh, G. J. 2006. Large-scale atmospheric circulation biases and changes in global climate model simulations and their importance for climate change in Central Europe. *Atmos. Chem. Phys.* **6**, 863–881.